Digital Signal Processing 107 (2020) 102860

Contents lists available at ScienceDirect

Digital Signal Processing

www.elsevier.com/locate/dsp

A signal decomposition algorithm based on complex AM-FM model

De Zhu [a], Qingwei Gao [b,*], Yixiang Lu [b], Dong Sun [b]

[a] School of Computer Science and Technology, Anhui University, Hefei 230601, China
[b] School of Electrical Engineering and Automation, Anhui University, Hefei 230601, China

ARTICLE INFO

Article history:
Available online 23 September 2020

Keywords:
Signal processing
Time-frequency analysis
Adaptive model decomposition
Complex AM-FM model
Nonlinear multi-component signal

ABSTRACT

Model-based adaptive signal decomposition algorithm is an important research topic in the field of signal analysis. The amplitude modulated and frequency modulated (AM-FM) model is the most common model in the signal. In this paper, an adaptive signal decomposition algorithm based on the complex AM-FM model is proposed. This algorithm first obtains the analytical expression of the analyzed signal; and then the optimal equation of the analytic signal based on the model is realized by initializing the instantaneous frequency (IF) of the model. Finally, the partial differential equation and the alternating direction method of multipliers technique are used to solve the optimization equation to achieve a high precision estimation of the model. Experiments on simulated and real-life data verify that the proposed algorithm can accurately estimate the instantaneous amplitude (IA) and IF of each component in the signal, and has strong robustness and high efficiency.

1. Introduction

A large number of the signals generated by natural or artificial systems (e.g. seismic signals, speech signals, radar signals and mechanical bearing signals) can be expressed as the sum of the models. In the past few decades, many researchers have invested in the research of multi-component signal decomposition algorithms, and have created many novel and effective algorithms. These methods can be grouped into two categories: the time-frequency analysis (TFA) methods and the mode-based optimization methods.

The most common TFA algorithm is short-time Fourier transform (STFT) and wavelet transform, as well as extension algorithms based on these algorithms. For example, synchrosqueezing transform (SST) enhances the time-frequency (TF) resolution based on the traditional TFA and realizes the recombination of the signal [1,2]. Besides, many scholars have proposed high-order SST [3] and multisynchrosqueezing transform [4] to improve the accuracy of instantaneous frequency (IF). The synchroextracting transform (SET) [5] and local maximum synchrosqueezing transform [6] are based on the STFT to maximum reserve the time-frequency information of the energy concentration region in the signal, and then extract the instantaneous frequency trajectory and signal component. However, these algorithms can not achieve a high-precision estimation of signal models due to Heisenberg uncertainty principle.

The empirical mode decomposition (EMD) [7] is the first proposed data-driven mode optimization algorithm, and then many EMD-based extension algorithm and applications are proposed, such as Empirical mode decomposition (EEMD) [8,9], multivariate empirical mode decomposition (MEMD) [10,11], bidimensional empirical mode configuration (BEMD) [12]. However, the EMD-based algorithm lacks strict mathematical proof, and cannot solve the mode-mixing problem. In 2014, the optimal segmentation algorithm based on spectrum bandwidth, known as the variational mode decomposition (VMD) [13], was proposed to implement the decomposition of the signal. Subsequently, many algorithms, such as two-dimensional variational mode decomposition [14], complex variational mode decomposition (CVMD) [15] and multivariate variational mode decomposition (MVMD) [16], have been proposed and applied to engineering [17,18]. Nevertheless, VMD correlation algorithm cannot realize the decomposition of the signal which contains the cross-order components. Null space pursuit (NSP) is an operator-based algorithm for signal decomposition [19]. Peng and other scholars design a variety of operators for different models and decompose the signal into the form of a series of narrow-band modes by iterative operation [20–22]. This algorithm has high algorithm complexity and is not suitable for online processing.

Vold-Kalman filter order tracking (VKF-OT) algorithm using the Vold-Kalman filter with the weight to achieve the separation of components in the signal, even the cross-order components [23,24]. The algorithm is to get the traced order of components by minimizing the error energy of the structural and data equations by the least square method. As a result, this algorithm has a high algorithm complexity, which is more suitable for process-

* Corresponding author.
E-mail address: qingweigao@ahu.edu.cn (Q. Gao).

https://doi.org/10.1016/j.dsp.2020.102860
1051-2004/

ing offline jobs. Therefore, the adaptive VKF-OT is proposed by Pan [25,26], which simplifies the computational complexity and makes it considered in engineering. However, the detection accuracy of this algorithm is based on the premise of the IF accuracy of the signal, which is obtained by STFT from the signal. Therefore, the accurate calculation of IF is very important for the calculation accuracy of VKF-OT [27].

Chirp signal mode is also a common signal mode in nature. The chirp signal can be seen as a linear and nonlinear frequency modulation (FM) signal whose instantaneous frequency varies linearly with time. In recent years, signal analysis algorithms based on chirp mode can be noted. [28,29] propose the parameter estimation algorithm of single and multi-components based on chirp mode respectively. The correlation application based on chirp mode is also proposed [30,31].

In this paper, an adaptive signal decomposition algorithm based on a complex AM-FM model (ASD-CAMFM) is proposed. The proposed algorithm can decompose the signal into the sum of several AM-FM models by cyclic iteration. The algorithm cannot only converge quickly but also extract the instantaneous amplitude (IA) and IF parameters of each AM-FM mode accurately.

The remainder of this paper is organized as follows. Section 2 describes the mathematical model of AM-FM and the review of Hilbert Transform (HT) [32]. Section 3 devoted to the principle and implementation of the proposed method. The performance of the algorithm is verified by experiments in Section 4, and Section 5 completes the paper.

2. Background

2.1. AM-FM model

In this paper, the AM-FM model is a prerequisite for the proposed algorithm derivation, so we define it as follows.

Definition 1. In a broad sense, the IA and IF of the AM-FM signal vary with time, and the frequency of IA is much lower than IF of the model. The model of AM-FM is denoted as follows:

$$x(t) = A(t)\cos(2\pi f(t)t + \theta), \tag{1}$$

where $A(t)$ is IA of $x(t)$, $f_{IF}(t) = f(t) + f'(t)t$ is IF of $x(t)$ and θ denotes the initial phase. We define f_a is IF of $A(t)$. In addition, the model satisfies the following conditions:

(1) $A(t)$ and $f_{IF}(t)$ have continuous derivatives.
(2) Both $A(t)$ and $f_{IF}(t)$ are non-negative.
(3) $f_a << f_{IF}(t)$ and $(f_{IF}(t))' << f_{IF}(t)$.

In general, the signal is not composed of a single component, but of several AM-FM components. In addition, the signal is usually disturbed by the noise. Thus, the multicomponent model signal is defined as follows:

$$s(t) = \sum x_i(t) + n(t), \tag{2}$$

where $x_i(t)$ is an AM-FM signal components and $n(t)$ is environmental noise (Gaussian or non-Gaussian noise).

2.2. Hilbert transform

HT of the real signal $x(t) = A(t)\cos(2\pi f(t)t + \theta)$, which has Fourier Transform (FT), is defined as

$$x_H(t) = x(t)\frac{1}{\pi t}. \tag{3}$$

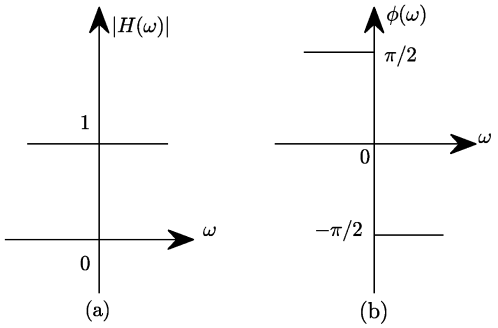

Fig. 1. Amplitude and phase spectrum of HT. (a) The amplitude spectrum of HT; (b) the phase spectrum of HT.

And the equivalent FT of HT is

$$H(\omega) = -j\mathrm{sgn}(\omega) = |H(\omega)|\exp(j\varphi(\omega)). \tag{4}$$

From the above, it can be seen that HT is an ideal bandwidth phase-shift filter, and $x_H(t)$ is the orthogonal signal of $x(t)$. The amplitude and phase spectrum of HT are shown in Fig. 1. Besides, HT requires the signal to satisfy Bedrosian theorem (BT) [32]. BT required that the analyzed signal be satisfied: both the IA and IF of the model are slowly varying. Thus, Definition 1 is consistent with BT. Then $x(t)$ has the following analytic formula:

$$\begin{aligned} x_A(t) &= x(t) + jx_H(t) \\ &= A(t)\exp(j2\pi f(t)t + \theta), \end{aligned} \tag{5}$$

where $x_H(t)$ is HT of $x(t)$.

3. Proposed algorithm

In this section, we mainly discuss the framework of ASD-CAMFM. Through the introduction of the previous section, it can be seen that the main work of signal decomposition based on the AM-FM model is to estimate the IA and IF parameters of the model. In the following sections, we will focus on how to implement the parameter estimation of the AM-FM model through the proposed framework.

3.1. Algorithmic principles

There is an AM-FM signal, whose analytical form is shown in (5). The purpose of the proposed algorithm is to estimate the IA and IF of the model. Suppose we've estimated IF of the model at t is $\hat{f}(t)$, thus formula can be written as follows:

$$\begin{aligned} x_A(t) &= A(t)\exp(j2\pi f(t)t + \theta) \\ &= A(t)\exp(j2\pi(f(t) - \hat{f}(t))t)\cdot\exp(j2\pi\hat{f}(t)t + \theta) \\ &= P(t)\cdot Q(t), \end{aligned} \tag{6}$$

where $P(t) = A(t)\exp(j2\pi(f(t) - \hat{f}(t))t)$ and $Q(t) = \exp(j2\pi\hat{f}(t)t + \theta)$.

Thus, we have decomposed the analytic formula of the signal into the form of multiplication of two subcomponents. When $\hat{f}(t) = f(t)$, then $P(t) = A(t)$ and $Q(t) = \exp(j2\pi f(t)t + \theta)$. Thus, the amplitude modulated (AM) and frequency modulated (FM) components of model are separated by using the estimated frequency. Then we equate the solution of the model to the following optimization problems

$$\begin{aligned} &\min_{\left\{P(t),\hat{f}(t)\right\}} \left\{\|T(P(t))\|_2^2\right\}, \\ &s.t. \quad \|x_A(t) - P(t)\cdot Q(t)\|_2^2 \le \varepsilon, \end{aligned} \tag{7}$$

where ε is the upper bound of the estimated residuals, T can be a second-order differential operator a higher-priced operator, which is determined by $A(t)$. In order to ensure the fast tracking of IA, the third-order differential operator is selected in this paper as follows:

$$T = \begin{bmatrix} -1 & 3 & -3 & 1 & 0 & 0 & \cdots & 0 \\ 0 & -1 & 3 & -3 & 1 & 0 & \cdots & 0 \\ \vdots & \ddots & \ddots & \ddots & \ddots & \ddots & \ddots & \vdots \\ 0 & \cdots & 0 & -1 & 3 & -3 & 1 & 0 \\ 0 & \cdots & 0 & 0 & -1 & 3 & -3 & 1 \end{bmatrix}. \tag{8}$$

For the above optimization problems, we can convert to the following Lagrange optimization function:

$$\Gamma(P, Q) = \|T(P(t))\|_2^2 + \lambda(\|P(t) * Q(t)(1+\upsilon) - x_A(t)\|_2^2), \tag{9}$$

where λ is the Lagrange multiplier and υ is the leak factor which indicates the proportion of the model remaining in the remaining component.

The above optimization problem is a multi-parameter convex optimization problem. We use partial differential equations (PDEs) and alternating direction method of multipliers (ADMM) to realize the iterative solution of parameters. The iterative formulas of parameters are calculated as follows:

$$Q_i(t) = \exp(j2\pi \hat{f}_i(t)t), \tag{10}$$

$$P_i(t) = \left(\frac{T^H T}{\lambda} + Q_i(t)^H Q_i(t)(1+\upsilon)\right)^{-1} Q_i(t)^H x_A(t), \tag{11}$$

where i is the number if iterations, $(\cdot)^H$ denotes the conjugate transpose operation and $\hat{f}_i$ is the i-th estimated IF.

Therefore, the formula for estimated complex AM-FM model is

$$\hat{x}_{Ai}(t) = P_i(t) \cdot Q_i(t). \tag{12}$$

In addition, there are two parameters (υ and λ) in the optimization formula that need to be optimized in the calculation. Firstly, we discuss the optimization strategy for the leak factor υ.

Here, we defined that $x = \hat{x} + u$, $\hat{x}$ is the estimated component and u is the residual component. Thus, $\hat{x}$ and u are mutually orthogonal signals: $\langle \hat{x}, u \rangle = 0$. However, if the model is not fully decomposed in the calculation, the leakage υ of the model component is leaked in the residual. Therefore $\hat{x}^H x / \hat{x}^H \hat{x} = 1 + \upsilon$, so the optimization formula of υ is:

$$\upsilon_i = \frac{\hat{x}_i(t)x(t)}{\hat{x}_i(t) * \hat{x}_i(t)} - 1. \tag{13}$$

The Lagrange multiplier λ is the bridge between the constraints and the objective function in the equilibrium optimization equation, and its optimization performance directly determines the convergence speed of the algorithm. As the optimization equation is iteratively advanced, the estimated model is closer to the real signal. Referring to Equation (9), the constraint on the second part is weakened, while the constraint of the model increases accordingly. Therefore, the convergence process of λ should be decreasing.

Substituting Equations (11) into Equation (12), then

$$\begin{aligned} \hat{x}_{Ai}(t) &= \left(\frac{T^H T}{\lambda} + Q_i(t)^H Q_i(t)(1+\upsilon)\right)^{-1} Q_i(t)^H x_A(t) \cdot Q_i(t) \\ &= \frac{1}{\lambda}\left(\left(\frac{T^H T}{\lambda^2} + \frac{1}{\lambda} Q_i(t)^H Q_i(t)(1+\upsilon)\right)^{-1} Q_i(t)^H Q_i(t)\right) \\ &\quad \cdot x_A(t). \end{aligned} \tag{14}$$

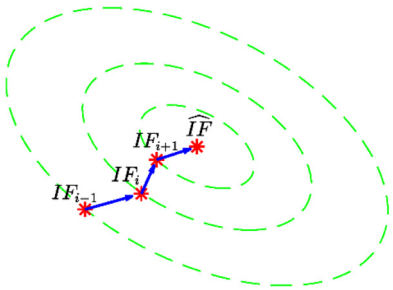

Fig. 2. Iterative schematic of IF.

We define $K_i(Q_i, \upsilon, \lambda) = (T^H T/\lambda^2 + 1/\lambda \cdot Q_i(t)^H Q_i(t)(1+\upsilon))^{-1} Q_i(t)^H Q_i(t)$, thus, $\lambda_i = x_A(t)/\hat{x}_{Ai}(t) \cdot K_i(Q_i, \upsilon, \lambda)$. When $\hat{f}(t) \to f(t)$, $Q_i(t)$ approximates a stable exponential function, and λ and υ in the formula are slowly changing variables. We can consider $K_i(Q_i, \upsilon, \lambda)$ to be a slowly varying value. Therefore, we can estimate the following equation: $\lambda_i/\lambda_{i+1} \approx \hat{x}_{i+1}/\hat{x}_i \approx 1 + \upsilon$. Thus, the estimated iteration formula of λ as:

$$\lambda_{i+1} = \frac{\lambda_i}{1+\upsilon}. \tag{15}$$

3.2. IF initialization and update

From the above algorithm derivation, it is known that the premise of the successful implementation of the proposed algorithm is the selection of the initial IF, and the optimization problem must be a convex problem, as shown in Fig. 2. These two issues can also be summarized as:

(1) The initial value of any point of IF must be within the convex set of its optimal value.

(2) The frequency update of IF must be a convex optimization problem.

The initialization problem of IF is realized by many methods, such as traditional STFT. In this paper, we use SET algorithm to estimate the signal IF in order to improve the detection accuracy of the weak component [5]. We set $s(t) = A \cdot \cos(jf_0 t)$, and its frequency expression is $\hat{s}(\xi) = 2\pi A \cdot \delta(\xi - f_0)$. We add a Gaussian window to the signal and perform STFT operation to obtain the following formula:

$$\begin{aligned} G(t, f) &= \int_{-\infty}^{+\infty} g(u-t)s(t)\exp(-jfu)du \\ &= A \cdot \hat{g}(f-\xi)\exp(jf_0 t). \end{aligned} \tag{16}$$

We assume that $s(t)$ has a component at $\tilde{t}$ time and its IF is $\tilde{f}$, then the real part of $G(\tilde{t}, \tilde{f})$ is positive and also the local extreme point of the neighborhood. We perform partial derivative calculations on time t for the above formula, and then obtain IF estimation formula:

$$f_t(t, f) = -j\frac{\partial_t G(t, f)}{G(t, f)}, \tag{17}$$

where ∂_t is the partial differential operator of time.

Thus, if $f_t(t, f) < 0.5\Delta\omega$ ($\Delta\omega$ is the frequency resolution), there is an instantaneous frequency f in the signal at t time. We can estimate all IF components present in the signal by this method.

In order to prevent the influence of other factors on the algorithm, the update of IF is very important. The estimation error of the IF can be obtained by $P_i(t)$. We define the frequency error of the i-th as $\Delta f_i = f(t) - \hat{f}_i(t)$, then $\tan(2\pi \Delta f_i t) = imag(P_i(t))/real(P_i(t))$. So the update formula of IF is:

$$\hat{f}_{i+1}(t) = \hat{f}_i(t) + \frac{1}{2\pi}\partial_t(\arctan(imag(P_i(t))/real(P_i(t)))). \quad (18)$$

From Definition 1, we can know that the IF of AM-FM is smooth. However, the IF and error frequency calculated by (17)-(18) are not smooth. In order to ensure the smooth approximation of the signal model, the initial value of the IF and Δf_i are low-pass filtered [33]:

$$\tilde{f} = (\frac{1}{\mu}T_2^H T_2 + I)f, \quad (19)$$

where T_2 the second-order differential operator and μ is used to limit the cut-off frequency of the filter. In this paper, we set $\mu_0 = 1e-6$. Of course, it can also be set to a smaller value to ensure higher frequency smoothness.

3.3. Proposed signal decomposition algorithm

The proposed algorithm is a complex AM-FM model decomposition algorithm in the complex domain. In order to extract the AM-FM component of the signal, the detected signal is firstly to converted into analytical form by HT, and the amplitude modulation component $P(t)$ and fundamental frequency component $Q(t)$ of the AM-FM model are estimated by IF that extracted by SET; then, the updated IF of component is obtained by (18). In addition, the optimization parameters λ and υ are updated according to the intermediate results in the algorithm. At the same time, the algorithm has a strong saw-tooth phenomenon in the process of IF estimation. Therefore, low-pass filter processing is used to ensure the smoothness of IF in this paper. The optimal solution of the method is obtained by iterative optimization. From the principle of algorithm, we can understand that the proposed algorithm as an improved complex-version of the adaptive chirp mode pursuit algorithm (ACMP) [29].

In summary, the calculation flow of ASD-CAMFM is proposed as follows:

Algorithm 1: ASD-CAMFM for single component extracting.

Step1: The analytic signal of $S(t)$; and Initialize λ, υ, μ and topping threshold ε.
Step2: Calculation IF by formulas (16) and (17).
Step3: Get $P_i(t)$ and $Q_i(t)$ by formulas (10) and (11).
Step4: Obtain the model components real($x_i(t)$) from formula (12).
Step5: Iterative parameters λ_i and υ_i are updated by formulas (13) and (15), respectively.
Step6: Updating IF by formulas (18) and (19).
Step7: If $\|x_i(t) - x_{i-1}(t)\|_2^2 / \|x_i(t)\|_2^2 < \varepsilon$, then stop; else $i = i+1$, go Step2.

The computational cost of this algorithm mainly reflects the calculation of matrix. Assuming the dimension of the signal is $1 \times n$, then the dimension of $P(t)$ and $Q(t)$ are $1 \times n$. The multiplication of the $n \times n$ matrix is most used in the proposed algorithm. The computational cost of two-dimensional matrix multiplication is $O(n^{2.3728639})$ [34]. Assuming that the algorithm is iterative m time, the complexity of the algorithm is $O(m^* n^{2.3728639})$. It can be seen that the complexity of this algorithm is closely related to the length of the signal and the number of iterations.

For a signal with multiple components, the proposed algorithm can be called several times to realize the sequential decomposition of signal components. The process of the multi-component signal decomposition is as follows:

There are four parameters in the whole algorithm: λ, υ, μ and ε. ε is the topping threshold used to constrain the detection accuracy of the model; μ is used to constrain the filtering performance of the low pass filter, and the value of which is proportional to the truncation frequency of the filter. λ and υ are the optimization parameters of the Lagrange optimization function. In addition,

Algorithm 2: ASD-CAMFM for multiple components extracting.

Step1: The analytic signal of $S(t)$; and Initialize λ, υ, μ and topping threshold ε.
Step2: Set $i = 0$, $v_i = 0$, $u_i = S$.
Step3: Estimated the initial $\left\{\tilde{f}_i\right\}_{i=1,2\cdots}$ of signal by SET.
for $\left\{\tilde{f}_i\right\}_{i=1,2\cdots}$ do
Estimated parameters of model by ASD-CAMFM:
Model signal $v_i = \text{real}(x_i)$, IF(f_i) and IA (IA_i);
$u_{i+1} = u_i - v_i$, $i = i+1$.
end for
Output: signal models parameters: $\{v_i, f_i, IA_i\}_{i=1,2\cdots}$.

to ensure the robustness of optimization equation, the value of λ needs to be limited: *median* ($10\lambda_0$, λ_i, $0.1\lambda_0$). At the beginning of the algorithm, they are given initial values, and then they keep approaching the optimal solution by iteratively updating. In the paper, we set empirically there parameters as follows: $\lambda_0 = 1e-5$, $\upsilon_0 = 1e-2$, $\mu_0 = 1e-6$, $\varepsilon = 1e-7$.

3.4. Performance demonstration

To verify the performance of the proposed algorithm, we consider the following time-varying signal:

$$s(t) = (1 + 0.3\sin(2\pi \cdot 3t)) \cdot \sin(2\pi \cdot (50t + 2t^2 + 5\sin(1.2t)) + n(t), \quad (20)$$

where $n(t)$ is Gaussian white noise with SNR = 20. The IF of this signal is $50 + 4t + 6\cos(1.2t)$. The sampling frequency of the signal is 512 Hz and the signal lasts 3 s. Thus, the IF of the signal fluctuates in the range of 53.94-57.31 Hz.

To verify the accuracy of the method, we define the relative error (RE) for model estimation as follows:

$$RE = \frac{\|\tilde{x}(t) - x(t)\|_2}{\|x(t)\|_2}, \quad (21)$$

where $\tilde{x}(t)$ is the detection value and $x(t)$ is the theoretical value.

We first test the effect of the initial IF on algorithm stability. The center frequency of the real IF is known to be about 55 Hz. The IF initial value we set are constant values ranging from 40-70 Hz, intervals of 5 Hz. The detected results of IF and signal model are shown in Fig. 3, where Fig. 3(a) is the RE of the estimated IF for each iteration and Fig. 3(b) is the RE of the estimated model for each iteration. From the extraction results, it can be seen that the IF and signal model can basically converge within 5 iterations. In addition, the IF can be better approximated to the real values, and the model has a certain estimation error due to noise. From this test, it can be seen that the IF and signal model can be effectively detected when the initial IF distance is 15% different from the real values, that is, the algorithm does not require an accurate estimation of IF initial values.

Next, we test the effect of noise on algorithm performance. We first add noise with SNR 0 to 30 to the signal and then analyze it using the proposed algorithm. The results are shown in Fig. 4. From the results, it can be seen that noise has little effect on the estimation of IF, while it has a certain effect on the extraction of the signal model. From the RE of the extracted model, the RE of the model increases significantly when the SNR is lower than 5, and the algorithm still maintains a high detection accuracy when the SNR is greater than 15. It can be seen that the proposed algorithm has higher detection accuracy for signals with high SNR.

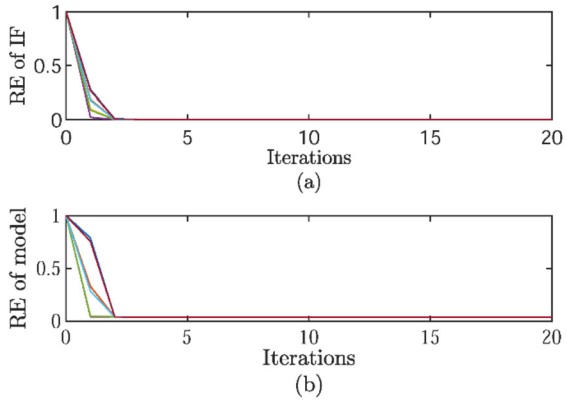

Fig. 3. Effecting of initial IF on detection accuracy. (a) RE of IF iterative trends, (b) RE of model iterative trends.

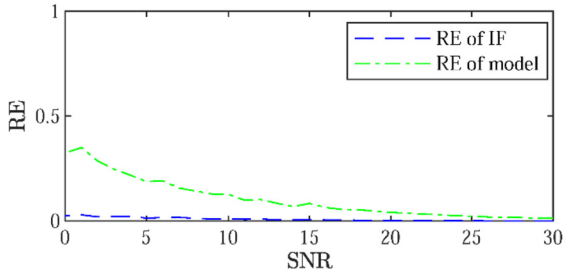

Fig. 4. RE of detection results for noisy signals with various SNR.

4. Experiment

In this section, some signals (artificial signals and natural signals) are used to verify the performance of the proposed algorithm. In addition, some conventional approaches, such as MSST [4], ACMP [29], VMD [13] and NSP-CD [22], are cited to comparative tests. The experiments of the paper are run under MATLAB R2018a with CPU Intel(R) Core(TM) i5-4460 and memory 8G.

4.1. Artificial signals

In this case, we consider a signal consisting of two time-varying components. This signal is defined as follows:

$$\begin{aligned} s_1(t) &= s_{m1}(t) + s_{m2}(t), \\ s_{m1}(t) &= (1 + 0.4\sin(2\pi \cdot 2t)) \cdot \sin(2\pi \cdot (80t + 3 \cdot \sin(1.2t)), \\ s_{m2}(t) &= (0.8 + 0.75\exp(-0.8t) + 0.2\sin(2\pi \cdot t)) \\ &\quad \cdot \sin(2\pi \cdot (130t + 2\sin(5t)). \end{aligned} \tag{22}$$

The sampling frequency is 512 Hz and the duration of the analyzed signal is 5 s. We can obtain the IAs of the two components: $1 + 0.4\sin(2\pi \cdot 2t)$ and $0.8 + 0.75\exp(-0.8t) + 0.2\sin(2\pi \cdot t)$, and IFs as $80 + 3.6\cos(1.2t)$ and $130 + 10\cos(5t)$, respectively. It can see that the IF and IA of the two components in the signal vary with time. The waveform and instantaneous frequency of the signal are shown in Fig. 5. Fig. 5(a) shows the waveform of the original signal, Fig. 5(b) shows the IF of the two components, and the waveforms of the two components are displayed in Fig. 5(c-d), respectively. From Fig. 5, it can be seen that the two components of the signal are periodic change waveform and decreasing subperiodic change waveform, respectively.

We first employ the proposed algorithm to decompose the signal, and the analysis results are shown in Fig. 6. Fig. 6(a-b) shows the IFs and IAs information of the extracted signal, and the detection results show that the algorithm can accurately track the IA

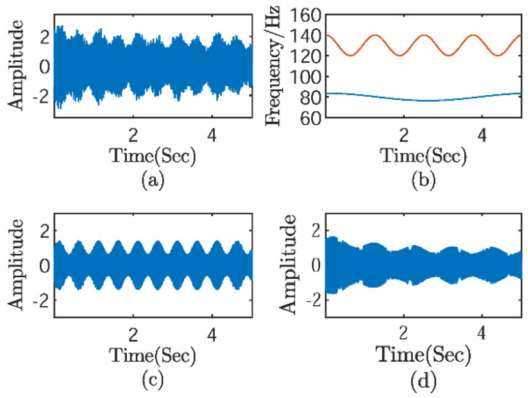

Fig. 5. Information of the artificial signals in Example 4.1. (a) Waveform of $s_1(t)$; (b) IFs of two components in signal, (c-d) Waveform of two components.

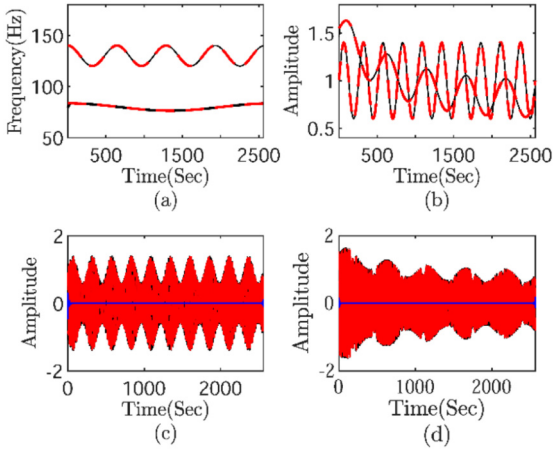

Fig. 6. Extracted results of Example 4.1 using proposed method. (a) IFs of Extracted model, (b) IAs of Extracted model, (c-d) two extracted models by proposed method (black line: the ideal waveform; red dotted line: the estimation information; blue line: estimated error). (For interpretation of the colors in the figure(s), the reader is referred to the web version of this article.)

and IF trajectory of the signal. From Fig. 6 (c-d), it can be seen that the estimation accuracy of this algorithm is very high except in the edge part. The estimation error in the signal edge is due to the HT of the signal when it is converted to a complex range.

For comparison, we list the extracted results of MSST, ACMP and VMD method as shown in Fig. 7. From the detection results, we can see that both components can be extracted by these algorithms. However, it is obvious that the higher accuracy was ACMD, followed by MSST, and finally by VMD. For a more accurate comparison of detection results, we use RE to measure the detection accuracy. RE of two extracted components by the proposed method are 0.02 and 0.009, respectively, and the RE of AMCD are 0.02 and 0.015. And, the iterations number of ACMD for two models are 72 and 12 iterations, while the proposed algorithm only needs 18 and 5 iterations. Thus, we can see that the proposed algorithm has a higher convergence speed than ACMD.

Besides, it can be seen that these algorithms have large detection errors at the signal edges. Now, we recalculate RE test results of the detection signal which have been removed the 128-edge sampling points (Length of windows), and the calculation results are shown in Table 1. The detection accuracy of the proposed algorithm reaches the number level of 10^{-4}, which is much higher than that of MSST and VMD. And the extraction accuracy of s_{m2} by ACMD is better than that of s_{m1}, so we can see that be seen that the ACMD has a weak detection accuracy for the signal with faster IA change.

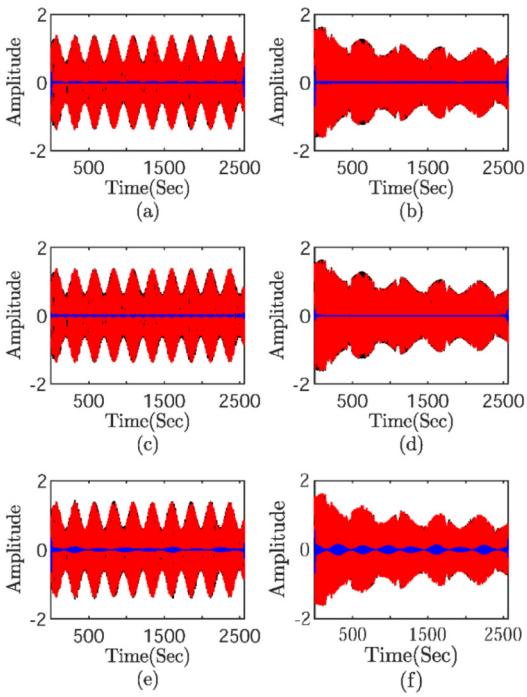

Fig. 7. Comparison experiment for model extraction in Example 4.1. (a-b) Extracted models by MSST, (c-d) extracted models by ACMD, (e-f) extracted models by VMD (black line: the ideal waveform; red dotted line: the estimation information; blue line: estimated error).

Table 1
Comparison experiment for model extraction with the proposed method and some publications.

Methods	MSST	ACMD	VMD	Proposed method
s_{m1}	$1.03 * 10^{-2}$	$1.84 * 10^{-2}$	$2.79 * 10^{-2}$	$4.4 * 10^{-4}$
s_{m2}	$1.18 * 10^{-2}$	$8.15 * 10^{-4}$	$6.94 * 10^{-2}$	$4.8 * 10^{-4}$

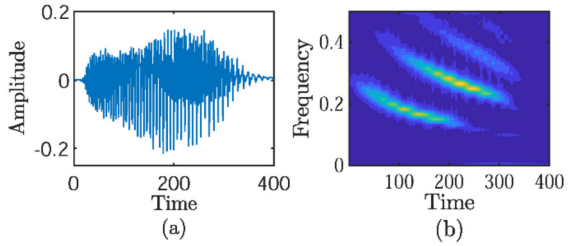

Fig. 8. Waveform and spectrum of bat signal. (a) The waveform of bat signal; (b) TFD of bat signal.

4.2. Natural signals: signals from animals

In this experiment, we focus on the decomposition of two kinds of signals from animals, which are bat signal and whale signals.

Now, the popular bat echolocation signal provided by Rice University is employed to illustrate the performance of the proposed algorithm [35]. The sampling period of this signal is 7 μs, and its length is 400 sampled points. The waveform and the TFD [36] of the signal are shown in Fig. 8. From Fig. 8(b), we can see that this

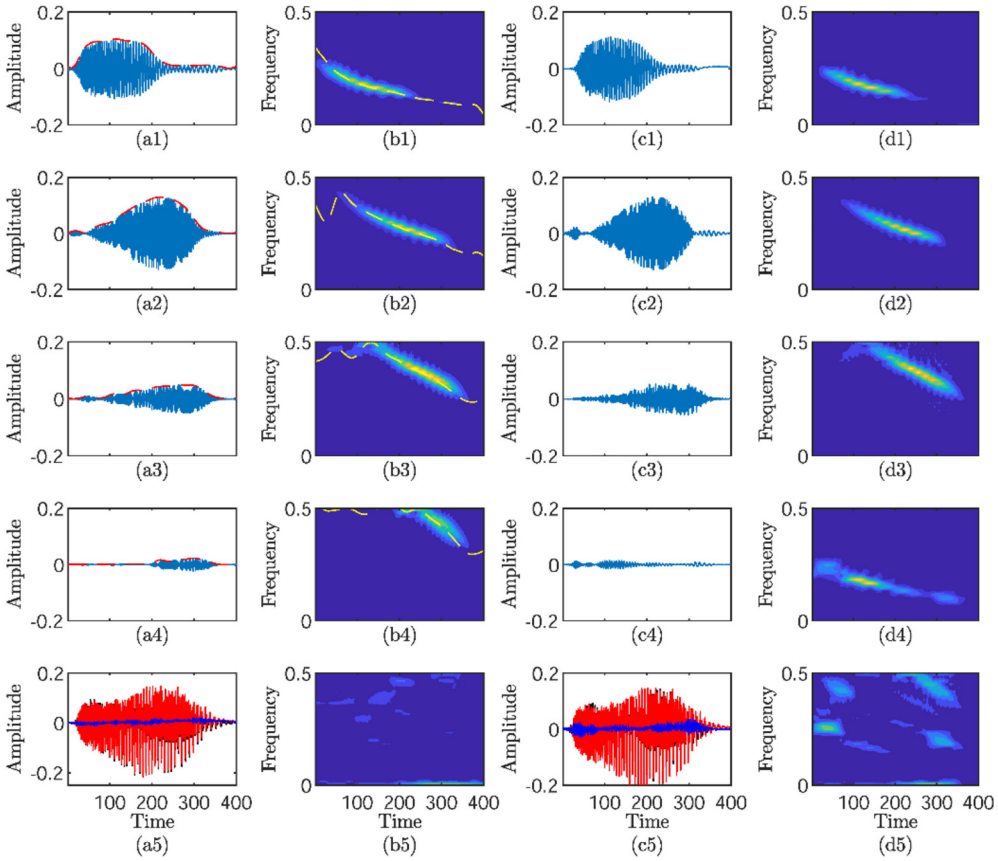

Fig. 9. Decomposed results of bat signal by proposed method and NSP-CD. (a1-a4) Waveform of extracted four models by the proposed method (red dotted line: the information of estimated IA); (b1-b4) corresponding TFD of a1-a4 (yellow dotted line: the information of estimated IF); (c1-c4) Waveform of extracted four models by NSP-CD; (d1-d4) corresponding TFD of c1-c4; (a5, b5) Waveform and TFD of residuals by the proposed method; (c5, d5) Waveform and TFD of residuals by NSP-CD (black line: the ideal waveform; red line: the estimation information; blue line: estimated error).

Table 2
Comparison experiment for algorithm complexity with the proposed method and NSP-CD.

Methods	Running time of *1-th*	Running time of *2-th*	Running time of *3-th*	Running time of *4-th*
NSP-CD	0.429 s	1.749 s	0.919 s	0.257 s
Proposed method	0.396 s	0.373 s	0.127 s	0.375 s

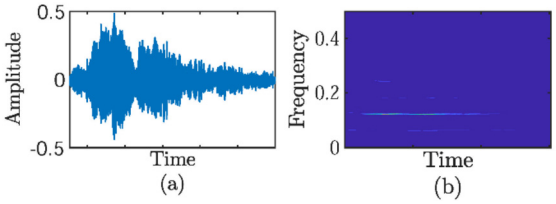

Fig. 10. Waveform and spectrum of whale signal. (a) The waveform of whale signal; (b) TFD of whale signal.

signal is composed of four components, all of which are the time-varying components, and these components overlap in the time domain.

To verify the effectiveness of the proposed algorithm, this experiment selected NSP-CD as a contrast test. NSP-CD is also a signal decomposition algorithm based on the complex-operator. We decompose the bat signal by the proposed algorithm and NSP-CD, and the decomposed results are displayed in Fig. 9. Fig. 9(a-b) shows the waveform and TFD of extracted models and residual signal by the proposed method. Meanwhile, the IA and IF information of the estimated models are also shown in the detection results. The decomposed models and residual information by NSP-CD are displayed in Fig. 9(c-d).

We can see from the decomposition results that the proposed algorithm can accurately decompose all components of the signal, and effectively estimate the IA and IF information of each component. From the estimation IF results, it can be seen that the IF estimation of the period with the small amplitude will be affected by the peripheral components and noise, which leads to the large IF fluctuation in the region. This problem can be improved by amending the μ. At the same time, from Fig. 9(a5, b5), residuals do not contain effective signal components, the extracted four signal models can effectively reconstruct the original signal. However, NSP-CD the algorithm did not accurately obtain the high-frequency components in the original signal at the fourth extraction, but extracted the residual components of the first component. From Fig. 9(c5, d5), we can see that the residual components extracted by NSP-CD contain weak energy model and the edge components of each model.

In this experiment, both algorithms realize the decomposition of signal model by cyclic iteration. The time required for the two

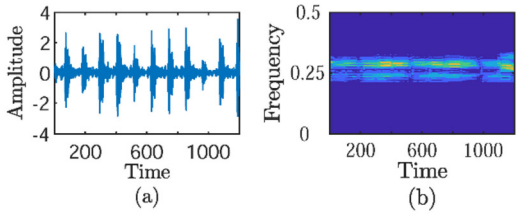

Fig. 12. Waveform and spectrum of bearing signal. (a) The waveform of the signal; (b) TFD of the signal.

algorithms to extract each model is shown in Table 2. From Table 2, we can see that the proposed algorithm is better than the NSP-CD (the fourth model extracted of NSP-CD by 0.257 s is invalid because of the wrong result).

From this experiment, we can see that the proposed algorithm is better than NSP-CD in terms of accuracy and efficiency, which also reflects that the proposed algorithm is an effective model decomposition algorithm.

Here we will use the proposed algorithm to analyze the whale signal from the coast of California, which is accompanied by high interference noise [37]. This signal is sampled at a sampling frequency of 11.025 kHz. In this experiment, the signal is intercepted for analysis, and its waveform and TFD are shown in Fig. 10. From Fig. 10(b), it can be seen that the whale signal is composed of one main component and three weak components. The decomposition results of the signal by the proposed algorithm are shown in Fig. 11. We can see from the decomposition results that the four components of the signal are effectively separated and the IA and IF of each model are accurately estimated. The amplitude of the principal component in the signal reaches 0.4, and the other three amplitudes are generally around 0.1. Furthermore, it can be seen that this whale signal is made up of four components, which have a constant IF.

4.3. Natural signals: bearing faults signals

In this example, we use the proposed algorithm to decompose the bearing fault signal and detect the bearing fault position. The bearing signal provided by the Bearing Data Center of Case Western Reserve University (CWRU) [38]. The bearing model is 6205-2RS JEM SKF with 0.007 inches diameter faults. The bearing signal is acquired by the accelerometers, which are placed at the drive end of the motor housing. The sampling frequency of this bearing signal is 12 kHz, and the rotation frequency of the bearing is 29.93 Hz. According to reference [39], the calculated fault frequency of this signal is 107.3 Hz.

In the experiment, we select the 1200 sampling point signal for analysis. The waveform and TFD of the signal are shown in Fig. 12. As shown in the figure, the fault signal is a time-varying signal with obvious amplitude-modulated characteristics, and the

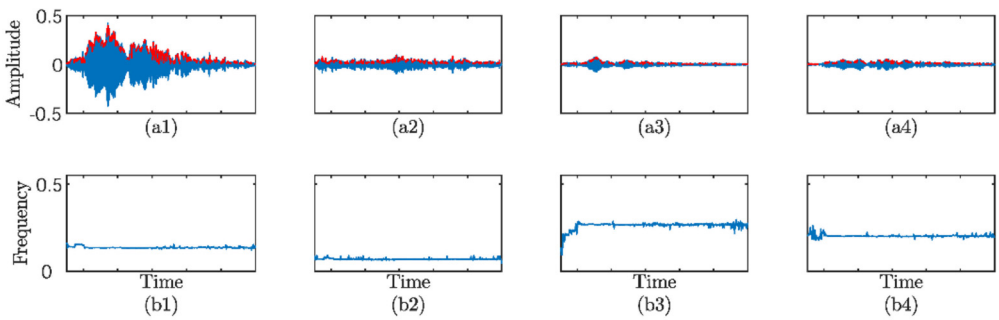

Fig. 11. Decomposed results of whale signal by proposed method. (a1-a4) Waveform of extracted four models by the proposed method; (b1-b4) corresponding TFD of a1-a4 (red dotted line: the information of estimated IA).

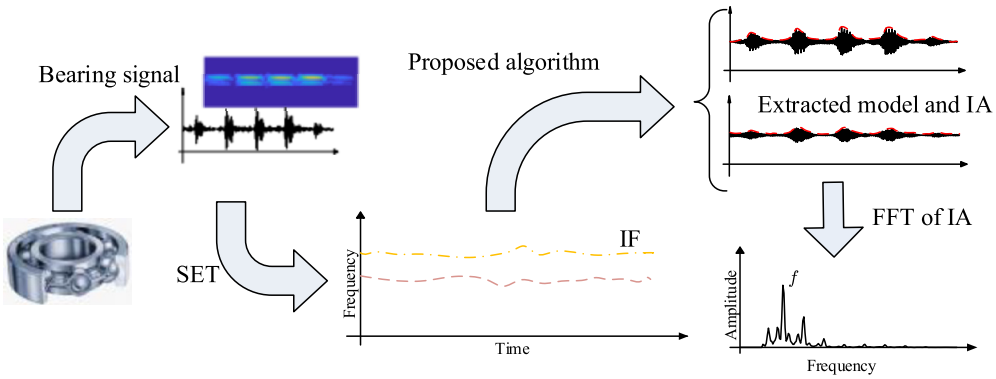

Fig. 13. Bearing Fault Detection Procession.

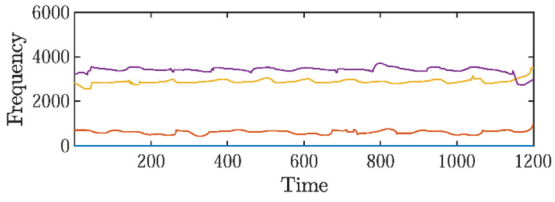

Fig. 14. Detected IFs of bearing signal by SET.

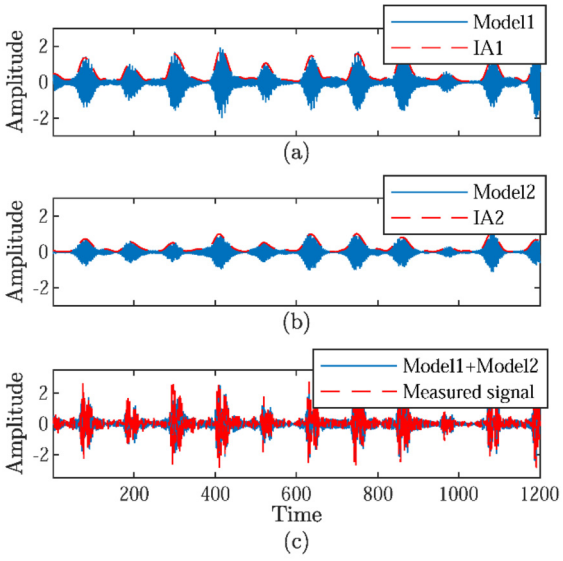

Fig. 15. Extracted results of bearing signal by proposed method. (a-b) Waveform of extracted two models (blue line: the extracted model; red dotted line: extracted IA); (c) Waveform of Reconstructed Signal (blue line: the sum of two extracted model; red dotted line: measured signal).

spectrum of the signal is mainly distributed in the range 2.5-4 kHz. From the above information, it is difficult to locate the bearing fault position.

In order to accurately extract the fault bearing signal model, this paper designs the following detection flow (see Fig. 13). Firstly, we estimate the IFs of the bearing signal by SET, as shown in Fig. 14. From the Fig. 14, we can see that this signal contains three main components, which are distributed in the range of 200 Hz and 2.5-4 kHz, respectively. Combined with the TFD of bearing signal in Fig. 12, we selected IFs of the two components distributed in the range 2.5-4 kHz for extraction. The decomposed results by the proposed method are shown in Fig. 15. The extracted models and the corresponding IAs waveform are described in Fig. 15 (a)-(b), and the waveform of the sum of two models and the original signal waveform are displayed in Fig. 15(c). From the analysis we can see that the extracted model can reconstruct the original signal well. Lastly, we analyze the IA of the larger energy model to obtain the fault frequency of the vibration model, see Fig. 16. It can been seen that the fault frequency and the harmonic are detected accurately in Fig. 16. This example verifies that the proposed algorithm can accurately extract the fault model components of the fault bearing signal and accurately detect the fault frequency.

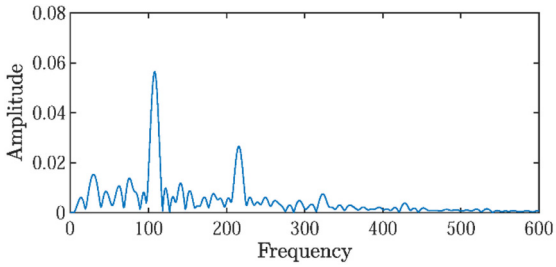

Fig. 16. Fault frequency detection result by proposed method.

5. Conclusions

In this paper, a novel signal adaptive decomposition algorithm based on AM-FM analytical model is proposed. The main contribution point of the paper are as follows: the AM-FM model decomposition framework of analytical signals, the estimation of initialization IF based on SET and the adaptive iteration of model parameters. The algorithm first estimates the IF components in the signal, and then solves the optimization equation of the model by optimizing iteration to estimate the IF and IA of the model, and finally to realize the extraction of the AM-FM model. In this paper, some simulation and real signal decomposition experiments are used to verify the effectiveness of this algorithm. At the same time, we also carry out comparative experiments with the state-of-art method (i.e., MSST, ACMD, VMD, NSP-CD) to verify the accuracy of the proposed algorithm.

It should be noted that the algorithm is suitable for the decomposition of the single component model. The multi-component model decomposition based on AM-FM analytical model, especially the model decomposition with cross components, has greater research value in engineering, which is our next research focus.

CRediT authorship contribution statement

Conception and design of study: De Zhu, Qingwei Gao, Yixiang Lu, Dong Sun. Algorithm implementation and testing: De Zhu, Dong Sun. Drafting the manuscript: De Zhu, Yixiang Lu. Writing: Review & Editing: De Zhu, Yixiang Lu. Revision of the manuscript: De Zhu, Yixiang Lu

Declaration of competing interest

The authors declared that they have no conflicts of interest to this work, and they do not have any commercial or associative interest that represents a conflict of interest in connection with the work submitted.

Acknowledgment

This work is supported by the Nature Science Foundation of Anhui (2008085MF183, 2008085MF192), the Key Science Program of Anhui Education Department (KJ2018A0012), the Research Fund for Doctor of Anhui University (J01003266), and is also supported by the National Natural Science Foundation of China (NSFC) (61370110, 61402004).

References

[1] I. Daubechies, J. Lu, H.T. Wu, Synchrosqueezed wavelet transforms: an empirical mode decomposition-like tool, Appl. Comput. Harmon. Anal. 30 (2) (2011) 243–261.
[2] F. Auger, et al., Time-frequency reassignment and synchrosqueezing: an overview, IEEE Signal Process. Mag. 30 (6) (2013) 32–41.
[3] X. Tu, Y. Hu, F. Li, S. Abbas, Z. Liu, W. Bao, Demodulated high-order synchrosqueezing transform with application to machine fault diagnosis, IEEE Trans. Ind. Electron. 66 (4) (2019) 3071–3081.
[4] G. Yu, Z. Wang, P. Zhao, Multisynchrosqueezing transform, IEEE Trans. Ind. Electron. 66 (7) (2019) 5441–5455.
[5] G. Yu, M. Yu, C. Xu, Synchroextracting transform, IEEE Trans. Ind. Electron. 64 (10) (2017) 8042–8054.
[6] G. Yu, Z. Wang, P. Zhao, Z. Li, Local maximum synchrosqueezing transform: an energy-concentrated time-frequency analysis tool, Mech. Syst. Signal Process. 117 (2019) 537–552.
[7] N.E. Huang, et al., The empirical mode decomposition and the Hilbert spectrum for nonlinear and non-stationary time series analysis, Proc. R. Soc. Lond. Ser. A Math. Phys. Eng. Sci. 454 (1971) (1998) 903–995.
[8] Z. Wu, N.E. Huang, Ensemble empirical mode decomposition: a noise-assisted data analysis method, Adv. Adapt. Data Anal. 1 (1) (2009) 1–41.
[9] H. Liu, Q. Zhan, C. Yang, J. Wang, The multi-timescale temporal patterns and dynamics of land surface temperature using ensemble empirical mode decomposition, Sci. Total Environ. 652 (2019) 243–255.
[10] N. Ur Rehman, D.P. Mandic, Filter bank property of multivariate empirical mode decomposition, IEEE Trans. Signal Process. 59 (5) (2011) 2421–2426.
[11] Y. Zheng, G. Xu, Quantifying mode mixing and leakage in multivariate empirical mode decomposition and application in motor imagery–based brain-computer interface system, Med. Biol. Eng. Comput. 57 (6) (2019) 1297–1311.
[12] C.-Y. Chen, S.-M. Guo, W. Chang, J.S.-H. Tsai, K.-S. Cheng, An improved bidimensional empirical mode decomposition: a mean approach for fast decomposition, Signal Process. 98 (2014) 344–358.
[13] K. Dragomiretskiy, D. Zosso, Variational mode decomposition, IEEE Trans. Signal Process. 62 (3) (2014) 531–544.
[14] K. Dragomiretskiy, D. Zosso, Two-dimensional variational mode decomposition, in: Energy Minimization Methods in Comput. Vis. Pattern Recognit., 2015, pp. 197–208.
[15] Y. Wang, F. Liu, Z. Jiang, S. He, Q. Mo, Complex variational mode decomposition for signal processing applications, Mech. Syst. Signal Process. 86 (2017) 75–85.
[16] N.U. Rehman, H. Aftab, Multivariate variational mode decomposition, IEEE Trans. Signal Process. 67 (23) (2019) 6039–6052.
[17] W. Wang, C. Pan, J. Wang, Multi-component variational mode decomposition and its application on wall-bounded turbulence, Exp. Fluids 60 (6) (2019) 1–16.
[18] Z. Feng, et al., Monthly runoff time series prediction by variational mode decomposition and support vector machine based on quantum-behaved particle swarm optimization, J. Hydrol. 583 (2020) 1–12.
[19] S. Peng, W. Hwang, Null space pursuit: an operator-based approach to adaptive signal separation, IEEE Trans. Signal Process. 58 (5) (2010) 2475–2483.
[20] X. Hu, S. Peng, W.L. Hwang, Multicomponent AM-FM signal separation and demodulation with null space pursuit, Signal Image Video Process. 7 (6) (2013) 1093–1102.
[21] X. Hu, S. Peng, W.L. Hwang, Adaptive integral operators for signal separation, IEEE Signal Process. Lett. 22 (9) (2015) 1383–1387.
[22] S.P.X.H. Baokui Guo, P. Xu, Complex-valued differential operator-based method for multi-component signal separation, Signal Process. 132 (Supplement C) (2017) 66–76.
[23] M.C. Pan, Y.F. Lin, Further exploration of Vold-Kalman-filtering order tracking with shaft-speed information—I: theoretical part, numerical implementation and parameter investigations, Mech. Syst. Signal Process. 20 (5) (2006) 1134–1154.
[24] M.-C. Pan, Y.-F. Lin, Further exploration of Vold–Kalman-filtering order tracking with shaft-speed information—II: engineering applications, Mech. Syst. Signal Process. 20 (6) (2006) 1410–1428.
[25] M.-C. Pan, C.-X. Wu, Adaptive Vold–Kalman filtering order tracking, Mech. Syst. Signal Process. 21 (8) (Nov. 2007) 2957–2969.
[26] M.-C. Pan, W.-C. Chu, D.-D. Le, Adaptive angular-velocity Vold–Kalman filter order tracking – theoretical basis, numerical implementation and parameter investigation, Mech. Syst. Signal Process. 81 (2016) 148–161.
[27] T. Liu, Z. Luo, J. Huang, S. Yan, A comparative study of four kinds of adaptive decomposition algorithms and their applications, Sensors (Switzerland) 18 (7) (2018).
[28] S. Chen, Z. Peng, Y. Yang, X. Dong, W. Zhang, Intrinsic chirp component decomposition by using Fourier series representation, Signal Process. 137 (January) (2017) 319–327.
[29] S. Chen, Y. Yang, Z. Peng, X. Dong, W. Zhang, G. Meng, Adaptive chirp mode pursuit: algorithm and applications, Mech. Syst. Signal Process. 116 (2019) 566–584.
[30] J. Niu, G. Ning, Y. Shen, S. Yang, Detection and identification of cutting chatter based on improved variational nonlinear chirp mode decomposition, Int. J. Adv. Manuf. Technol. 104 (5–8) (2019) 2567–2578.
[31] S. Chen, X. Dong, G. Xing, Z. Peng, W. Zhang, G. Meng, Separation of overlapped non-stationary signals by ridge path regrouping and intrinsic chirp component decomposition, IEEE Sens. J. 17 (18) (2017) 5994–6005.
[32] E. Bedrosian, A product theorem for Hilbert transforms, Proc. IEEE 74 (3) (1962) 520–521.
[33] M.P. Tarvainen, P.O. Ranta-aho, P.A. Karjalainen, An advanced detrending method with application to HRV analysis, IEEE Trans. Biomed. Eng. 49 (2) (2002) 172–175.
[34] F. Le Gall, Powers of tensors and fast matrix multiplication, in: Proc. Int. Symp. Symb. Algebr. Comput. ISSAC, 2014, pp. 296–303.
[35] https://cpb-us-e1.wpmucdn.com/blogs.rice.edu/dist/0/7717/files/software/batsignal.zip.
[36] F. Hlawatsch, G.F. Boudreaux-Bartels, Linear and quadratic time-frequency signal representations, IEEE Signal Process. Mag. 9 (2) (1992) 21–67.
[37] Discovery of sound in the sea, [Online]. Available, https://dosits.org/resources/resource-categories/feature-sounds/haunting-refrains-humpback/, 2002.
[38] Case western reserve university bearing data center, http://csegroups.case.edu/bearingdatacenter/pages/welcome-case-western-reserve-university-bearing-data-center-website.
[39] N. Tandon, A. Choudhury, A review of vibration and acoustic measurement methods for the detection of defects in rolling element bearings, Tribol. Int. 32 (8) (1999) 469–480.

De Zhu was born in Anhui, China, in 1987. He received the B.S. degree in electrical engineering, Anhui University, Hefei, in 2010, and the M.S. degree in pattern recognition from Anhui University in 2013. He is currently pursuing the Ph.D. degree in pattern recognition at Anhui University. His research interest is primarily in the area of signal processing.

Qingwei Gao was born in Anhui, China, in 1965. He received the Ph.D. degree in information and communication engineering from the University of Science and Technology of China, in 2002. He is currently a Professor with the School of Electrical Engineering and Automation, Anhui University. His research interests include wavelet analysis, image processing, and fractal signal processing.

Yixiang Lu was born in Anhui, China, in 1980. He received the B.S. degree in measurement control and instrumentation, the M.S. degree in detection technology and automatic equipment, and the Ph.D. degree in circuits and systems from Anhui University in 2004, 2007, and 2015, respectively. His research interests include wavelet analysis, image processing, and statistical signal processing.

Dong Sun was born in Anhui, China, in 1983. He received the B.S. degree from the automation department of Anhui University in 2003, the M.S. degree in pattern recognition from the Anhui University in 2006, and the Ph.D. degree in computer science and application from Anhui University in 2016. His current research interest is primarily in the area of sparse representation, fractal, and image restoration.